Phase diagram of the t-U-J_1-J_2 chain at half filling

X. Huang,[1] E. Szirmai,[2] F. Gebhard,[1] J. Sólyom,[2] and R. M. Noack[1]
[1]*Fachbereich Physik, Philipps-Universität Marburg, D-35032 Marburg, Germany*
[2]*Research Institute for Solid State Physics and Optics, P.O. Box 49, H-1525 Budapest, Hungary*
(Received 20 March 2008; revised manuscript received 23 May 2008; published 25 August 2008)

We investigate the Hubbard chain at half band filling with additional nearest-neighbor and next-nearest-neighbor spin exchange J_1 and J_2 using bosonization and the density-matrix renormalization group. For $J_2=0$ we find a spin-density-wave phase for all positive values of the Hubbard interaction U and the Heisenberg exchange J_1. A frustrating spin exchange J_2 induces a bond-order-wave phase. For some values of J_1, J_2, and U, we observe a spin-gapped metallic Luther-Emery phase.

DOI: 10.1103/PhysRevB.78.085128 PACS number(s): 71.10.Fd, 71.10.Hf, 71.30.+h, 74.20.Mn

I. INTRODUCTION

The Hubbard chain is the archetype of one-dimensional strongly correlated electron systems. At half band filling and for all values of the Hubbard interaction U, it exhibits insulating spin-density-wave (SDW) behavior, marked by a critical behavior of the spin correlations. In a weak-coupling picture, this insulating behavior is generated by umklapp scattering, while in strong coupling, the opening of the Mott-Hubbard gap leads to behavior of the spin degrees of freedom governed by an effective Heisenberg chain. These perturbative results are reinforced by the exact Bethe-Ansatz solution.[1] Hubbard-type models are relevant to a wide variety of quasi-one-dimensional materials such as polymers,[2] strontium cuprates,[3] or the charge transfer salt TTF-TCNQ.[4]

One important experimental question is to what extent the spin correlations remain critical when additional interactions are present. It is well known that any dimerization or sufficiently large frustration can lead to a spin gap in the Heisenberg-type spin models. A nearest-neighbor Coulomb repulsion,[5,6] an alternating local potential,[7,8] or a second-neighbor hopping[9,10] can lead to a spin gap in models for itinerant interacting electrons.

The Hubbard model with a nearest-neighbor antiferromagnetic exchange in two dimensions is of interest in the context of the high-T_c cuprates. In particular, spin-liquid states[11] and gossamer superconductivity[12] at and near half filling have been proposed as necessary precursors to high-temperature superconductivity at higher doping. Since it is not clear whether such states are present in sufficient strength and for sufficiently wide parameter regimes in the pure Hubbard or t-J models, additional interactions, including a spin exchange, have been proposed to be relevant.[13]

In this work, we investigate the effect of two additional terms on the phase diagram of the Hubbard chain at half-band filling (average electron occupation $\langle n\rangle=1$), namely, explicit antiferromagnetic exchange interactions between nearest neighbors and between next-nearest neighbors.

The Hamiltonian is given by

$$H=-t\sum_{i,\sigma}(c^{\dagger}_{i,\sigma}c_{i,\sigma}+\text{H.c.})+U\sum_{i}n_{i,\uparrow}n_{i,\downarrow}+J_1\sum_{i}\boldsymbol{S}_i\boldsymbol{S}_{i+1}+J_2\sum_{i}\boldsymbol{S}_i\boldsymbol{S}_{i+2}, \quad (1)$$

where $c^{\dagger}_{i,\sigma}$ ($c_{i,\sigma}$) creates (annihilates) an electron with spin σ at site i, $n_{i,\sigma}=c^{\dagger}_{i,\sigma}c_{i,\sigma}$, and $\boldsymbol{S}_i$ is the spin operator on site i: $S^{\alpha}_i=\frac{1}{2}\sum_{\sigma,\sigma'}c^{\dagger}_{i,\sigma}\hat{\sigma}^{\alpha}_{\sigma,\sigma'}c_{i,\sigma'}$. The indices $\alpha=x$, y, z, and $\hat{\sigma}^{\alpha}_{\sigma,\sigma'}$ are the Pauli matrices. Here t is the hopping amplitude and U the strength of the on-site Coulomb interaction. The antiferromagnetic Heisenberg parameters J_1 and J_2 correspond to nearest- and next-nearest-neighbor exchange, respectively. Note that additional weak hopping amplitudes $t_2,t_3\ll t$ to next-nearest and next-next-nearest neighbors do not change the physics qualitatively; see Sec. II A.

The unfrustrated ($J_2=0$) version of this model has previously been investigated both analytically and numerically. In particular, a generalized model with an anisotropic Heisenberg coupling was investigated in Ref. 14 using bosonization. While this work concentrated primarily on the case of ferromagnetic exchange, isotropic antiferromagnetic exchange was included in a phase that is marked as "dimer long-range order," which corresponds to a bond-order wave (BOW) in our notation; see below. The phase diagram from bosonization of the isotropic antiferromagnetic exchange was considered explicitly in Refs. 15 and 16, supported by numerical calculations using the transfer-matrix renormalization group[15] (TMRG) and exact diagonalization.[16] The phase diagram found contains two phases: a bond charge-density-wave phase (our BOW phase) at sufficiently small U for all J_1 and a SDW at larger U. The critical value of U_c goes to zero at small and large J_1 and reaches a maximum value $U_c/t\approx 0.35$ at intermediate J_1. Our model also covers limiting cases of more elaborate models, e.g., for superconductivity in one-dimensional materials.[17]

In this work, we re-examine the bosonization treatment of the t-U-J_1 model in the weak-coupling regime, including the renormalization of the coupling constants within the mean-field approximation. In addition, we consider the effect of the additional frustrating exchange J_2, which allows us to explicitly induce the bond-order phase and to make contact with the known phase diagram of the frustrated Heisenberg chain at large U. We also carry out high-precision ground-state density-matrix renormalization group (DMRG) calculations, which allow us to explore the phase diagram numerically exactly. Both the revised bosonization and the DMRG calculations indicate that a BOW phase is not present for $J_2=0$; the system is in a SDW phase for *all* positive J_1 and U. We show that a BOW phase can be induced by turning on J_2 positively, with the critical value required depending on U

and J_1. At larger values of J_2, we find additional phases including a spin-gapped metallic phase which we identify as a Luther-Emery phase.

The paper is organized as follows: In Sec. II, we discuss the bosonization calculation and the resulting phase diagram. Section III contains our numerical DMRG results and compares and contrasts the behavior obtained with that predicted by bosonization. In Sec. IV, we discuss the overall phase diagram of the model in terms of the results from the two methods as well as the implications of our findings.

II. FIELD THEORY

We start our investigation with an analytical treatment of our model for small couplings $U, J_1, J_2 \ll t$. For simplicity, we take $\hbar \equiv 1$ everywhere.

A. Linearization of the spectrum

In terms of fermion operators the Hamiltonian (1) has the form

$$H = -t\sum_{i,\sigma}(c^{\dagger}_{i,\sigma}c_{i,\sigma} + \text{H.c.}) + U\sum_{i} c^{\dagger}_{i,\uparrow}c_{i,\uparrow}c^{\dagger}_{i,\downarrow}c_{i,\downarrow} + \sum_{\ell=1}^{2}\frac{J_\ell}{4}\sum_{i}[2(c^{\dagger}_{i,\downarrow}c_{i,\uparrow}c^{\dagger}_{i+\ell,\uparrow}c_{i+\ell,\downarrow} + c^{\dagger}_{i,\uparrow}c_{i,\downarrow}c^{\dagger}_{i+\ell,\downarrow}c_{i+\ell,\uparrow}) + c^{\dagger}_{i,\uparrow}c_{i,\uparrow}c^{\dagger}_{i+\ell,\uparrow}c_{i+\ell,\uparrow} + c^{\dagger}_{i,\downarrow}c_{i,\downarrow}c^{\dagger}_{i+\ell,\downarrow}c_{i+\ell,\downarrow} - c^{\dagger}_{i,\uparrow}c_{i,\uparrow}c^{\dagger}_{i+\ell,\downarrow}c_{i+\ell,\downarrow} - c^{\dagger}_{i,\downarrow}c_{i,\downarrow}c^{\dagger}_{i+\ell,\uparrow}c_{i+\ell,\uparrow}]. \quad (2)$$

For low temperatures and for excitations at low energies, it is enough to consider a restricted Hilbert space which contains only states close to the Fermi surface. In one dimension, the Fermi surface consists only of two points $k = \pm k_F$. In the weak-coupling limit, additional hopping terms to next-nearest and next-next-nearest neighbors modify the Fermi velocity but do not change the physics qualitatively as long as there are only two Fermi points. Therefore, we have not considered these terms explicitly in Hamiltonian (1).

Around the Fermi points, the spectrum can be linearized and one can introduce left-moving and right-moving fermions corresponding to the states near $-k_F$ and $+k_F$, respectively,

$$c_{i+\ell,\sigma} \to c_{i+\ell,\sigma,+}e^{ik_F(R_i+\ell a)} + c_{i+\ell,\sigma,-}e^{-ik_F(R_i+\ell a)}, \quad (3)$$

for $\ell = 0, 1, 2$. Here R_i is the coordinate vector of the site i and a is the lattice constant. For the half-filled system, $k_F = \pi/2a$. Therefore, the left- and right-moving fermions have the phase factor $e^{\pm i\ell\pi/2}$ for different values of ℓ. When written in terms of the chiral fermions $c_{i+\ell,\sigma,\pm}$, each interaction term of Hamiltonian (2) splits into four new terms. Two of them correspond to forward-scattering processes whose couplings are denoted by g_2 and g_4 in standard g-ology notation.[18] In addition, there are two backward-scattering processes which describe "true" backward scattering (g_1 processes) and umklapp scattering (g_3 processes). Due to the SU(2) symmetry of the spin sector, all processes depend only on the relative spins of the scattering electrons. This is denoted by the subscripts $\parallel$ and $\perp$ if the scattering electrons have the same or opposite spins, respectively. The relations between the g-ology parameters and the couplings of our original model are

$$g_{1\perp} = U - J_1/2 - 3J_2/2, \quad (4a)$$

$$g_{2\perp} = U + J_1/2 - 3J_2/2, \quad (4b)$$

$$g_{3\perp} = U + 3J_1/2 - 3J_2/2, \quad (4c)$$

$$g_{4\perp} = U - 3J_1/2 - 3J_2/2, \quad (4d)$$

and

$$g_{1\parallel} = -J_1/2 + J_2/2, \quad (5a)$$

$$g_{2\parallel} = J_1/2 + J_2/2, \quad (5b)$$

$$g_{3\parallel} = -J_1/2 + J_2/2, \quad (5c)$$

$$g_{4\parallel} = J_1/2 + J_2/2. \quad (5d)$$

In order to analyze the low-energy g-ology model, we apply the bosonization method.

B. Bosonization of the Hamiltonian

First, we introduce the continuous chiral fermion fields $\psi_{\sigma,\pm}(x)$ by making the replacement $c_{i,\sigma,\pm}/\sqrt{a} \to \psi_{\sigma,\pm}(x)$. The bosonization of the on-site interaction is straightforward. Using Abelian bosonization, we introduce the chiral boson phase fields $\phi_{\sigma,\pm}(x)$ via

$$\psi_{\sigma,\pm}(x) = \frac{1}{\sqrt{2\pi}}F_{\pm}e^{\pm i2\phi_{\sigma,\pm}(x)}, \quad (6)$$

where $F_{\pm}$ are the so-called Klein factors which ensure the anticommutation relations of the fermion fields. The symmetric and antisymmetric combinations of the spin-dependent boson fields $\phi_{c,\pm} = \phi_{\uparrow,\pm} + \phi_{\downarrow,\pm}$ and $\phi_{s,\pm} = \phi_{\uparrow,\pm} - \phi_{\downarrow,\pm}$ correspond to the collective charge and spin modes, respectively.

In order to bosonize the nonlocal processes, one must expand the fermion fields with respect to the lattice constant. The bosonized form of the g-ology Hamiltonian density, up to leading order in the expansion with respect to the lattice constant, is

$$H^{(0)}(x) = \frac{1}{2\pi}\sum_{r=\pm}[v_\rho(\partial_x\phi_{c,r})^2 + v_\sigma(\partial_x\phi_{s,r})^2] + \frac{g_\rho}{2\pi^2}(\partial_x\phi_{c,+}) \times (\partial_x\phi_{c,-}) - \frac{g_c}{2\pi^2}\cos(2\phi_c) - \frac{g_\sigma}{2\pi^2}(\partial_x\phi_{s,+})(\partial_x\phi_{s,-}) + \frac{g_s}{2\pi^2}\cos(2\phi_s) - \frac{g_{cs}}{2\pi^2}\cos(2\phi_c)\cos(2\phi_s). \quad (7)$$

Here $\phi_{c/s} = \phi_{c/s,+} + \phi_{c/s,-}$ are the total phase fields, and the couplings are given by

$$g_\rho = g_{2\perp} + g_{2\parallel} - g_{1\parallel} = U + 3J_1/2 - 3J_2/2, \quad (8a)$$

$$g_\sigma = g_{2\perp} - g_{2\parallel} + g_{1\parallel} = U - J_1/2 - 3J_2/2, \tag{8b}$$

$$g_c = g_{3\perp} = U + 3J_1/2 - 3J_2/2, \tag{8c}$$

$$g_s = g_{1\perp} = U - J_1/2 - 3J_2/2, \tag{8d}$$

$$g_{cs} = g_{3\parallel} = -J_1/2 + J_2/2. \tag{8e}$$

The renormalized Fermi velocities are $v_\rho = 2t + (g_{4\parallel} + g_{4\perp})/2\pi$ and $v_\sigma = 2t + (g_{4\parallel} - g_{4\perp})/2\pi$. Here and in the following, we use the lattice constant as the unit for the coupling constants as well as for the Fermi velocities.

The spin-charge coupling term with coupling constant g_{cs} describes umklapp scattering processes between electrons with the same spin. This interaction term formally occurs in the lowest order of the expansion of the fermion fields with respect to the lattice constant. It is clear, however, that $g_{3\parallel}$ type processes can give contributions only for nonlocal interactions. Moreover, this spin-charge coupling term breaks the global spin SU(2) symmetry of the system. Therefore, in order to preserve this symmetry, and in order to treat the nonlocal interactions in a consistent way, the next-to-leading terms have to be taken into account in the expansion of the fermion fields. To first order, among other contributions, three new spin-charge coupling terms appear in the Hamiltonian. We find that the spin and charge velocities are changed by the term $(-g_{1\parallel}/2)$, and the symmetry-restoring nonlocal interaction terms are given by

$$H^{(1)}(x) = \frac{g_{c\sigma}}{2\pi^2}(\partial_x\phi_{s,+})(\partial_x\phi_{s,-})\cos(2\phi_c) - \frac{g_{\rho s}}{2\pi^2}(\partial_x\phi_{c,+})(\partial_x\phi_{c,-})\cos(2\phi_s) + \frac{g_{\rho\sigma}}{2\pi^2}(\partial_x\phi_{c,+})(\partial_x\phi_{c,-})(\partial_x\phi_{s,+})(\partial_x\phi_{s,-}). \tag{9}$$

The first two terms correspond to backward and umklapp scattering, respectively, between electrons with opposite spins, and the third term describes backward-scattering processes between electrons with equal spins. Initially, all these couplings are equal to g_{cs},

$$g_{\rho s} = g_{c\sigma} = g_{\rho\sigma} = g_{cs} = -J_1/2 + J_2/2. \tag{10}$$

The SU(2) symmetry of the spin sector assures $g_s = g_\sigma$, $g_{cs} = g_{c\sigma}$, and $g_{\rho s} = g_{\rho\sigma}$. Therefore, there are five independent couplings which we choose to be g_ρ, g_c, g_s, g_{cs}, and $g_{\rho s}$. We note that the renormalization of the Fermi velocities, which is a secondary effect, will not be taken into account in the following.

C. Renormalization-group analysis for fluctuating charge and spin fields

The Hamiltonian $H = H^{(0)} + H^{(1)}$ cannot be solved exactly. However, a renormalization-group (RG) analysis permits the investigation of the relative importance of the various couplings. In the RG procedure, the couplings are considered to be a function of some scaling parameter y, e.g., the logarithm of the effective bandwidth. As the scaling parameter is taken to infinity, the flow of the couplings shows which of them are important and which can be ignored, depending on whether or not they tend to zero, to a finite value, or to infinity. For example, when all couplings but the forward-scattering terms tend to zero, the Hamiltonian H describes a Luttinger liquid with freely propagating charge and spin degrees of freedom.

The one-loop RG equations for our five dimensionless running coupling constants $\tilde{g}_x(y) \equiv g_x(y)/4\pi t$ read[15,19]

$$\frac{d\tilde{g}_\rho(y)}{dy} = 2\tilde{g}_c^2 + \tilde{g}_{cs}^2 + \tilde{g}_s\tilde{g}_{\rho s}, \tag{11a}$$

$$\frac{d\tilde{g}_c(y)}{dy} = 2\tilde{g}_\rho\tilde{g}_c - \tilde{g}_s\tilde{g}_{cs} - \tilde{g}_{cs}\tilde{g}_{\rho s}, \tag{11b}$$

$$\frac{d\tilde{g}_s(y)}{dy} = -2\tilde{g}_s^2 - \tilde{g}_c\tilde{g}_{cs} - \tilde{g}_{cs}^2, \tag{11c}$$

$$\frac{d\tilde{g}_{cs}(y)}{dy} = -2\tilde{g}_{cs} + 2\tilde{g}_\rho\tilde{g}_{cs} - 4\tilde{g}_s\tilde{g}_{cs} - 2\tilde{g}_c\tilde{g}_s - 2\tilde{g}_c\tilde{g}_{\rho s} - 4\tilde{g}_{cs}\tilde{g}_{\rho s}, \tag{11d}$$

$$\frac{d\tilde{g}_{\rho s}(y)}{dy} = -2\tilde{g}_{\rho s} + 2\tilde{g}_\rho\tilde{g}_s - 4\tilde{g}_c\tilde{g}_{cs} - 4\tilde{g}_{cs}^2 - 4\tilde{g}_s\tilde{g}_{\rho s}, \tag{11e}$$

with initial values $\tilde{g}_x(y=0) = g_x/4\pi t$. From these equations, it follows that there is only a single line of weak-coupling fixed points, namely, $\bar{g}_c = \bar{g}_s = \bar{g}_{cs} = \bar{g}_{\rho s} = 0$. In order to show this, we note that we have started our analysis assuming that there is neither a charge gap nor a spin gap. This implies that a weak-coupling fixed point corresponds to $\bar{g}_c = \bar{g}_s = 0$. Equations (11a)–(11e) immediately imply that $\bar{g}_{cs} = \bar{g}_{\rho s} = 0$ also, and that only $\bar{g}_\rho$ remains undetermined.

A linear stability analysis of the fixed-point line shows that it is stable against small perturbations g_{cs} and $g_{\rho s}$, that it is marginally stable against small perturbations g_s and g_ρ, and that its stability with respect to perturbations g_c depends on the sign of the fixed-point value $\bar{g}_\rho$ (stable for $\bar{g}_\rho < 0$, unstable for $\bar{g}_\rho > 0$). Therefore, in order to determine the weak-coupling regime, it is convenient and sufficient to consider the RG equations without the spin-charge coupling terms, i.e., we may consider the RG equations for $\tilde{g}_{cs} = \tilde{g}_{\rho s} = 0$. We thus arrive at

$$\frac{d\tilde{g}_\rho(y)}{dy} = 2\tilde{g}_c^2, \tag{12a}$$

$$\frac{d\tilde{g}_c(y)}{dy} = 2\tilde{g}_\rho\tilde{g}_c, \tag{12b}$$

$$\frac{d\tilde{g}_s(y)}{dy} = -2\tilde{g}_s^2, \tag{12c}$$

in the vicinity of the weak-coupling fixed-point line.

This simpler problem is readily analyzed. The trajectory for the spin coupling $\tilde{g}_s(y)$ flows to infinity if $g_s<0$. In this case, a gap opens in the spin spectrum. If $g_s>0$, this coupling is marginally irrelevant, i.e., the spin mode remains soft. In the charge sector, $g_\rho=g_c$ initially, and this relation remains valid under the RG flow. Therefore, it is sufficient to consider Eq. (12a). It is seen that for $g_c>0$ the charge mode becomes gapped because $\tilde{g}_c(y)$ flows to infinity, otherwise the charge excitations remain gapless.

The simplified equations show that a fully gapless Luttinger-liquid phase $\bar{g}_c=\bar{g}_s=0$ is not possible for our model. The initial couplings would have to fulfill $g_c<0$ and $g_s>0$ which requires $J_2>2U/3+J_1$ for $g_c<0$ and $J_2<(2U-J_1)/3$ for $g_s>0$. These two conditions cannot be fulfilled simultaneously with positive bare couplings U, J_1, and J_2. Consequently, we must redo our RG analysis under the assumption that at least one of the two modes is gapped.

D. Renormalization-group analysis for gapped charge and/or spin modes

When one of the fields is gapped, the spin-charge coupling processes become relevant.[19,20] Their contribution will be considered on the mean-field level. In this picture, the gapped field is locked to a value which optimizes the interaction energy. Note that all bosonization treatments of a system with nonlocal interactions and a gap in either the spin or the charge sector are flawed when they neglect the renormalizations of the g-ology parameters which are generated by the locking of the spin and/or charge fields.[14–17]

When there is a gap in the charge sector, the charge field ϕ_c is locked at $\bar{\phi}_c=0$ mod π because the initial value of the coupling g_c is positive. Neglecting the fluctuations of the field ϕ_c in Hamiltonian (9), the terms proportional to $g_{\rho s}$ and $g_{\rho\sigma}$ do not contribute, and $\cos(2\phi_c)$ can be replaced by its weak-coupling mean-field value $\cos(2\phi_c)=1$. Due to this substitution, the interaction terms proportional to g_{cs} and $g_{c\sigma}$ become marginal because their scaling dimensions reduce to $\bar{x}_{cs}=\bar{x}_{c\sigma}=2$. On the mean-field level, the spin-coupling term proportional to g_{cs} is of the same form as the interaction term proportional to g_s in $H^{(0)}$. Therefore, the spin field ϕ_s fluctuates in the modified potential $g_s^*\cos(2\phi_s)$ with the new coupling g_s^*,

$$g_s^* = g_s - g_{cs} = U - 2J_2. \tag{13}$$

Analogously, the interaction term proportional to $g_{c\sigma}$ in $H^{(1)}$ combines with the interaction term proportional to g_σ in $H^{(0)}$ to produce the new coupling g_σ^*, with

$$g_\sigma^* = g_\sigma - g_{c\sigma} = U - 2J_2. \tag{14}$$

This equation shows that the SU(2) spin symmetry is preserved on the mean-field level.

In the presence of a charge gap and the SU(2) spin symmetry, we only have to analyze a single equation for $\tilde{g}_s$ instead of the five RG Eqs. (11a)–(11e), namely,

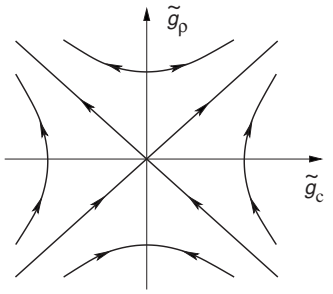

FIG. 1. Scaling curves for the charge-coupling parameters $\tilde{g}_c$ and $\tilde{g}_\rho$ in the presence of a spin gap.

$$\frac{d\tilde{g}_s(y)}{dy} = -2\tilde{g}_s^2, \tag{15}$$

with the initial value $\tilde{g}_s(y=0)=g_s^*/4\pi t$. It is readily seen that the spin mode becomes gapped if $g_s^*<0$, i.e., $J_2>U/2$, independently of the value of the nearest-neighbor interaction J_1.

When there is a gap in the spin sector, the spin field ϕ_s is locked at $\bar{\phi}_s=0$ mod π because the initial value of the coupling g_s is negative. Neglecting the fluctuations of the field ϕ_s in the Hamiltonian (9), the terms proportional to $g_{\rho\sigma}$ and $g_{c\sigma}$ do not contribute and $\cos(2\phi_s)$ can be substituted by its weak-coupling mean-field value $\cos(2\phi_s)=1$. Due to this substitution, the interaction terms proportional to g_{cs} and $g_{\rho s}$ become marginal because their scaling dimensions reduce to $\bar{x}_{cs}=\bar{x}_{\rho s}=2$. On the mean-field level, the charge-coupling term proportional to g_{cs} is of the same form as the interaction term proportional to g_c in $H^{(0)}$. Therefore, the charge field ϕ_c fluctuates in the modified potential $g_c^*\cos(2\phi_c)$ with the new coupling g_c^*,

$$g_c^* = g_c + g_{cs} = U + J_1 - J_2. \tag{16}$$

Using similar reasoning, the new coupling g_ρ^* becomes

$$g_\rho^* = g_\rho - g_{\rho s} = U + 2J_1 - 2J_2. \tag{17}$$

Note that these new initial couplings are *not* equal, so we must analyze the two-dimensional scaling curves defined by the equations

$$\frac{d\tilde{g}_\rho(y)}{dy} = 2\tilde{g}_c^2, \tag{18a}$$

$$\frac{d\tilde{g}_c(y)}{dy} = 2\tilde{g}_\rho\tilde{g}_c, \tag{18b}$$

given the initial values $\tilde{g}_c(y=0)=g_c^*/4\pi t$ and $\tilde{g}_\rho(y=0)=g_\rho^*/4\pi t$. The flow diagram is shown in Fig. 1.

The conditions for a gapped charge mode are either $g_\rho^*>0$ or $g_\rho^*<0$ and $|g_c^*|>|g_\rho^*|$. This leads to the result that a gapped charge mode exists if $J_2<2U/3+J_1$.

E. Phase diagram

In general, we find three regions where either the charge gap or the spin gap or both are finite. It is interesting to

analyze the dominant correlations in the various gapped phases. The order parameters for density waves in the charge (CDW), spin (SDW), bond-charge (BCDW), and bond-spin (BSDW) require the calculation of correlation functions using the operators

$$\mathcal{O}_{i,\mathrm{CDW}} = (-1)^i (n_{i,\uparrow} + n_{i,\downarrow}), \tag{19a}$$

$$\mathcal{O}_{i,\mathrm{SDW}} = (-1)^i (n_{i,\uparrow} - n_{i,\downarrow}), \tag{19b}$$

$$\mathcal{O}_{i,\mathrm{BCDW}} = (-1)^i (c^\dagger_{i,\uparrow} c_{i+1,\uparrow} + c^\dagger_{i,\downarrow} c_{i+1,\downarrow} + \mathrm{H.c.}), \tag{19c}$$

$$\mathcal{O}_{i,\mathrm{BSDW}} = (-1)^i (c^\dagger_{i,\uparrow} c_{i+1,\uparrow} - c^\dagger_{i,\downarrow} c_{i+1,\downarrow} + \mathrm{H.c.}), \tag{19d}$$

written in terms of the lattice fermions. These order parameters become

$$\mathcal{O}_{\mathrm{CDW}}(x) \propto \sin\,\phi_c(x) \cos\,\phi_s(x), \tag{20a}$$

$$\mathcal{O}_{\mathrm{SDW}}(x) \propto \cos\,\phi_c(x) \sin\,\phi_s(x), \tag{20b}$$

$$\mathcal{O}_{\mathrm{BCDW}}(x) \propto \cos\,\phi_c(x) \cos\,\phi_s(x), \tag{20c}$$

$$\mathcal{O}_{\mathrm{BSDW}}(x) \propto \sin\,\phi_c(x) \sin\,\phi_s(x), \tag{20d}$$

in bosonized form. When the charge mode is gapped, the field ϕ_c is locked at $\bar{\phi}_c = 0 \bmod \pi$. When the spin mode is gapped, the field ϕ_s is locked at $\bar{\phi}_s = 0 \bmod \pi$. Therefore, in the regime where both of the fields are gapped, we find that the BCDW order parameter is maximal. Therefore, the model describes a phase with bond ordering (BOW) for $\Delta_c \neq 0$ and $\Delta_s \neq 0$.

When only the charge mode is gapped, the spin field is a free field. However, upon increasing the scaling parameter (y) of the renormalization-group procedure, the initially negative spin coupling grows and tends to zero, and the spin field oscillates around $\pi/2$ (mod π). Therefore, for small couplings, the dominating ordering is SDW for $\Delta_c \neq 0$ and $\Delta_s = 0$. Note that the SU(2) spin symmetry is not spontaneously broken, i.e., the spin correlations are critical without true long-range order.

Similarly, when the spin mode is gapped and the charge mode is gapless, there is no true long-range charge order. Therefore, we call this phase the Luther-Emery (LE) phase. The charge coupling g_c tends to zero either from positive values or from negative values. Depending on the sign of the charge coupling, ϕ_c fluctuates around $\pi/2$ or around zero. Correspondingly, the dominating correlations are either CDW or BCDW for $\Delta_c = 0$ and $\Delta_s \neq 0$. The line which separates the dominant BCDW critical correlation and the dominant CDW correlations in the LE phase is indicated in Fig. 2 by a dashed line.

The resulting phase diagram of the t-U-J_1-J_2 model at weak coupling is shown in Fig. 2. For $U=0$, the spin gap is always finite for $J_2 > 0$. For $J_2 < J_1$, the charge gap is also finite, and the ground state is characterized by a bond-order wave. The charge gap closes at $J_2 = J_1$ and the system goes into a LE phase with no long-range ordering but critical charge-density-wave correlations.

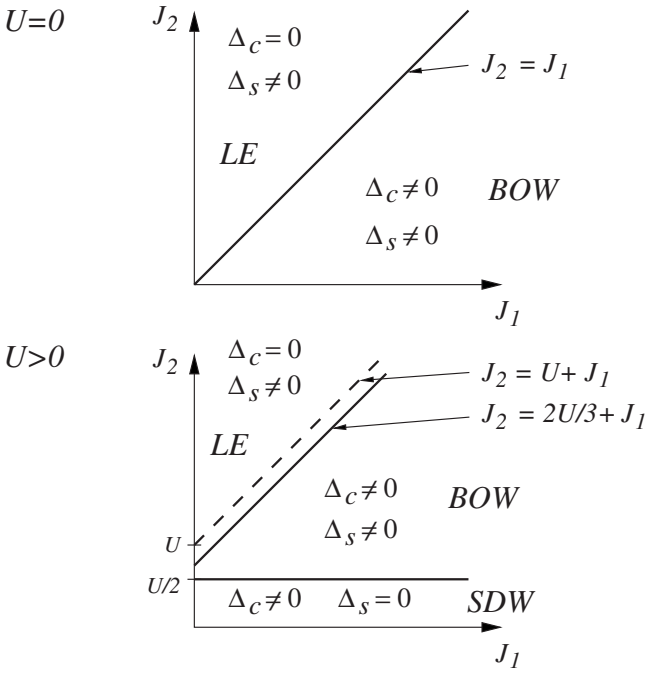

FIG. 2. Field-theory prediction for the half-filled t-U-J_1-J_2 model. The solid lines give the phase boundaries between the fully gapped regime (bond-order wave, BOW) and the semigapped regimes (spin-density wave, SDW; Luther-Emery, LE). The dashed line shows the border between dominantly charge-density-wave and bond-order-wave correlations in the Luther-Emery phase.

For $U > 0$, $J_1 > 0$, and $J_2 < U/2$, the ground state is analogous to the spin-density-wave phase of the one-dimensional Hubbard model, i.e., the charge gap is finite, the spin gap is zero, and the spin correlations are critical. For $2U/3 + J_1 > J_2 > U/2$, both the spin gap and the charge gap are finite. The ground state is a BOW with long-range order in the bond-charge-density-wave correlations. For $J_2 > 2U/3 + J_1$, the charge gap closes and the system goes over to the LE phase with a finite spin gap but no charge long-range order. For $2U/3 + J_1 < J_2 < U + J_1$, the bond-charge-density-wave fluctuations dominate, whereas, for $J_2 > U + J_1$, the fluctuations in the charge-density-wave order parameter are maximal.

In order to make contact with earlier work, we display the phase diagram of the t-U-J_1 model separately in Fig. 3. In contrast to previous results,[14–16] we do not find any signature of a BOW phase. For all $J_1 > 0$, the ground state is SDW, just as is the ground state of the half-filled Hubbard model for $U > 0$. This result is corroborated by our numerical DMRG data which we present in Sec. III.

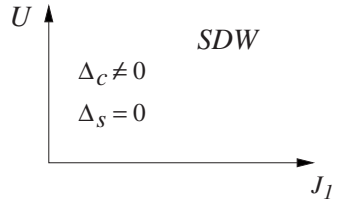

FIG. 3. Field-theory prediction for the half-filled t-U-J_1 model. For all $J_1 > 0$, the ground state is a spin-density-wave phase with a finite charge gap, zero-spin gap, and critical spin correlations.

III. NUMERICAL RESULTS

In order to explore the phase diagram of the Hamiltonian (1) and to test the predictions of bosonization, we carry out extensive, high-precision, ground-state DMRG calculations.[21–23] Relatively high sensitivity is required to resolve the phases especially in the weak-coupling regimes in which one would expect bosonization to be valid. In order to differentiate the possible phases, we calculate the spin gap Δ_s, the charge gap Δ_c, and the bond-order-wave parameter $\langle B\rangle$ of the one-dimensional t-U-J_1-J_2 model on lattices with open boundary conditions and up to $L=256$ sites. The weight of the discarded density-matrix eigenstates is held below a maximum of 10^{-9}.

For finite systems, the spin gap $\Delta_s(L)$ is defined as

$$\Delta_s(L) = E_0(L,L,S=1) - E_0(L,L,S=0). \tag{21}$$

Accordingly, the charge gap $\Delta_c(L)$ is determined using

$$\Delta_c(L) = [E_0(L,L+2,S=1) + E_0(L,L-2,S=0) - 2E_0(L,L,S=0)]/2, \tag{22}$$

where $E_0(L,N,S)$ is the ground-state energy for an L-site system with N electrons and total spin S. We extrapolate using second-order polynomials in $1/L$ to determine the spin gap Δ_s and the charge gap Δ_c in the thermodynamic limit,

$$\Delta_s(L) = \Delta_s^\infty + A_s/L + B_s/L^2,$$

$$\Delta_c(L) = \Delta_c^\infty + A_c/L + B_c/L^2, \tag{23}$$

where $\Delta_{c,s}^\infty$, $A_{c,s}$, and $B_{c,s}$ are fitting parameters. The staggered bond-order parameter is defined as

$$\langle B\rangle(L) = \frac{1}{2(L-1)} \sum_{i=1}^{L} \sum_{\sigma} (-1)^{i+1} \langle c_{i\sigma}^\dagger c_{i+1,\sigma} + \text{H.c.}\rangle. \tag{24}$$

Note that this order parameter would be identically zero for a finite translationally invariant system, e.g., one with periodic boundary conditions, but is nonvanishing for the open boundary conditions used here, which favor one of the two possible dimerization patterns. In order to determine if the phase is bond ordered in the thermodynamic limit, a finite-size extrapolation must be carried out. We extrapolate the bond-order parameter $\langle B\rangle$ using finite-size corrections of the form $1/L^\gamma$ without considering higher corrections

$$\langle B\rangle(L) = \langle B\rangle^\infty + A_B/L^\gamma, \tag{25}$$

where $\langle B\rangle^\infty$, A_B, and γ are fitting parameters. The fitting parameter γ is related to the form of the decay of the local bond-order parameter $\langle B_i\rangle = \langle c_{i\sigma}^\dagger c_{i+1,\sigma} + \text{H.c.}\rangle$ away from the boundaries; for critical decay this is governed by the relevant boundary critical exponent.[24] We find that adding higher-order terms, which increases the number of fit parameters, tends to make the fits less stable.

In the following, we first treat the t-U-J_1 model, i.e., $J_2=0$ in Hamiltonian (1), then study finite positive J_2, first with $U=0$ then with nonzero U. For simplicity, in the remainder of this article the energy scale is set by taking $t=1$, and so U, J_1, and J_2 are dimensionless quantities.

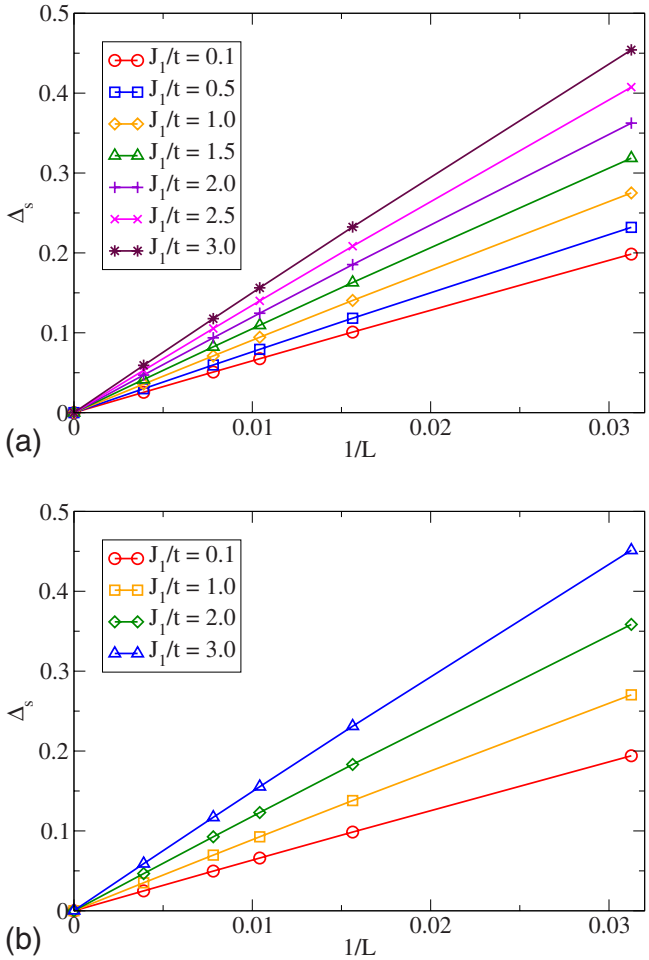

FIG. 4. (Color online) Finite-size extrapolation of the spin gap as a function of $1/L$ for the t-U-J_1 model at (a) $U=0$ and (b) $U=0.1$.

A. Results for $J_2=0$

For the unfrustrated case ($J_2=0$), our bosonization procedure of Sec. II predicts a SDW phase with a finite charge gap and critical gapless spin excitations $\Delta_c>0$ and $\Delta_s=0$. In the SDW phase, the bond-order parameter vanishes.

The finite-size extrapolation of the spin gap, plotted as a function of $1/L$ for $U=0$ and $U=0.1$, is shown in Fig. 4. As can be clearly seen, the scaling behavior is predominantly linear in $1/L$, and the $1/L\to 0$ extrapolated value Δ_s^∞ is zero on the scale of the plot for all values of J_1 for both values of U. A fit of the data with a second-order polynomial in $1/L$, as discussed above, yields a value of Δ_s^∞ that is less than 2×10^{-4} in all cases. This puts a rather stringent constraint on bond ordering in this case; the spin excitations are gapless to a very high numerical accuracy.

The system-size behavior of the charge gap is displayed in Fig. 5. As can be seen, the $1/L\to 0$ extrapolated value Δ_c^∞ is nonzero in general, with the scaling going from being predominantly linear in $1/L$ [with a small negative $(1/L)^2$ term] when Δ_c^∞ is small, to having a substantial positive $(1/L)^2$ term when Δ_c^∞ is significantly different from zero. Such finite-size behavior is typical for gaps in one-dimensional systems with open boundary conditions.

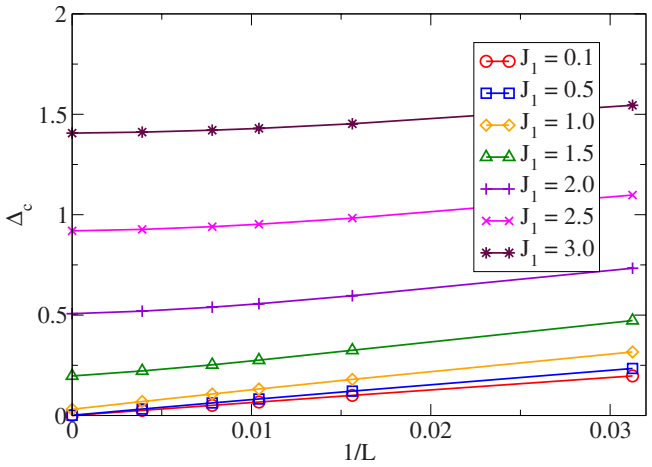

FIG. 5. (Color online) Finite-size extrapolation of the charge gap as a function of $1/L$ for the t-U-J_1 model at $U=0$.

The behavior of the extrapolated gaps as a function of J_1 is shown in Fig. 6. As discussed above, the spin gap is numerically indistinguishable from zero for all values of J_1 for both $U=0$ and $U=0.1$. The extrapolated charge gap is small on the scale of the plot for $J_1 \lesssim 0.8$, and then increases, crossing over to a linear increase for larger values of J_1. From bosonization, we would expect an exponential opening of the gap with J_1, similar to the exponential opening of the charge gap with U in the $J_1=0$ case.[25] The J_1 dependence of Δ_c^∞ in Fig. 6 is qualitatively consistent with such a behavior. We have not carried out an explicit fit because the detailed form of the exponential opening is not known from bosonization; to determine the specifics of a general exponential form via fitting to finite-size extrapolated data is difficult.

We now turn to the BOW order parameter, displayed as a function of J_1 for various system sizes and $L=\infty$ in Fig. 7. At each system size, $\langle B\rangle(L)$ has an appreciable positive finite value which varies significantly as a function of J_1. The $L\to\infty$ extrapolated value $\langle B\rangle^\infty$ is small, but still shows some variation with J_1. Note, however, that the extrapolated value is negative at small and large J_1 and is positive only for intermediate J_1. Taking the largest negative value ($\langle B\rangle^\infty \approx -0.003$) as a rough estimate of the extrapolation error, the

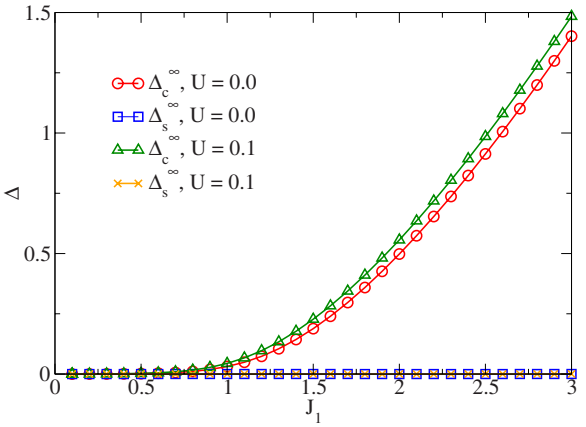

FIG. 6. (Color online) Extrapolated spin and charge gaps for the t-U-J_1 model at $U=0$ and $U=0.1$ as functions of J_1.

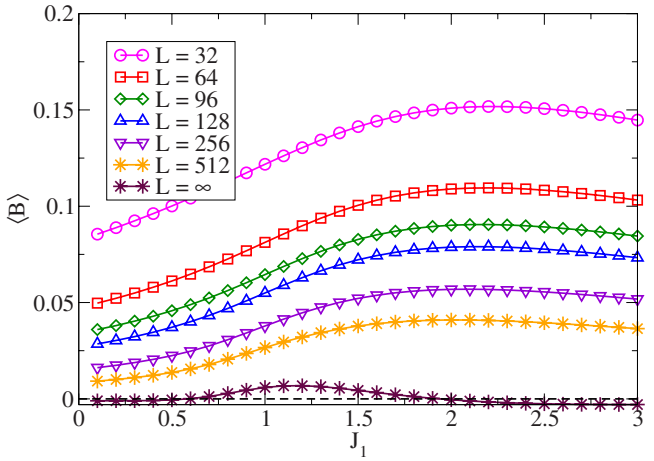

FIG. 7. (Color online) Bond-order parameter $\langle B\rangle(L)$ for $L=32,64,96,128,256,512$ and extrapolated bond-order parameter $\langle B\rangle^\infty$ as a function of J_1 for the t-U-J_1 model at $U=0$.

largest positive value $\langle B\rangle^\infty \approx 0.007$ is not distinguishable from zero to within our accuracy. Moreover the fit to Eq. (25) yields an exponent γ which varies between 0.47 and 0.77. All these underline the uncertainty in carrying out extrapolations using this analytic form and the sensitivity of $\langle B\rangle^\infty$ to the details of the fit. On the other hand, as discussed above, Δ_s^∞ vanishes to a high accuracy for all J_1, precluding a BOW phase. Thus, within the numerical methods applied here, the spin gap seems to be a significantly more sensitive probe for the existence of a bond-order-wave phase than the bond-order parameter $\langle B\rangle$ itself.

Our DMRG calculations for $J_2=0$ are thus in agreement with the predictions of the bosonization calculations of Sec. II; see Fig. 3: the ground-state phase is a SDW with gapless spin excitations for all positive U and J_1. While we have treated explicitly only two values of the interaction strength $U=0$ and $U=0.1$, we have chosen these values in accordance with the phase diagrams of Refs. 15 and 16 which predict the appearance of a bond-order-wave phase only for $U \lesssim 0.35$. At larger values of U, the behavior should be that of the ordinary half-filled Hubbard chain and one would not expect a BOW phase to occur.

B. Results for $U=0$ and nonzero J_2

We now include the explicit frustration J_2 while setting the on-site Coulomb interaction to zero.

Figure 8 shows the system-size extrapolated spin and charge gaps Δ_s^∞ and Δ_c^∞ as functions of J_2 at $U=0$ and $J_1=1$. (We do not show the finite-size extrapolation, which proceeds similarly to that in Figs. 4 and 5, explicitly.) The spin gap opens slowly at small J_2, but with a form consistent with a critical $J_2^s=0$ (see the inset in particular). The charge gap decreases rapidly with J_2 at small J_2, reaching zero at $J_2^{c(1)} \approx 1=J_1$, but then opens again at $J_2^{c(2)} \approx 2$. At weak coupling, this behavior of both gaps is consistent with the predictions of bosonization, but the reopening of the charge gap for larger J_2 is not contained in the bosonization analysis. However, such large values of J_2 are clearly outside its region of validity.

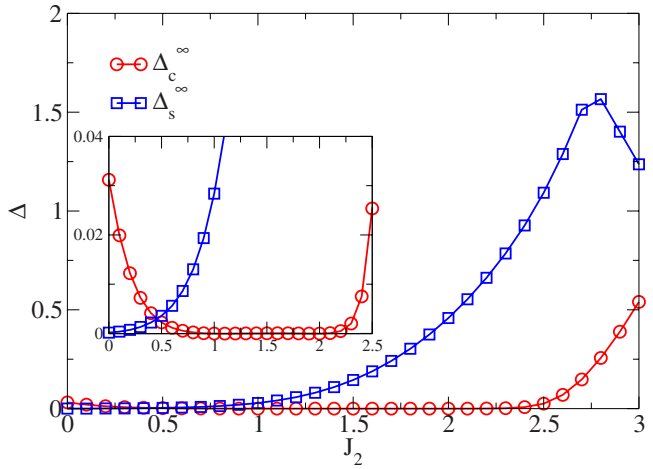

FIG. 8. (Color online) Extrapolated spin gap and charge gap as functions of J_2 for $U=0$, $J_1=1$. The inset displays the same data for $J_2 \leq 2.5$ on an enlarged scale.

Representative results for the finite-size scaling of the bond-order parameter $\langle B \rangle$ are present in Fig. 9. For small J_2, the scaling behavior is similar to that for $J_2=0$, yielding an exponent γ that varies between 0.44 and 0.71. However, for large J_2, the data extrapolate almost linearly to finite values. This illustrates that the scaling form Eq. (25) goes over to a function that might be better fit by a polynomial in $1/L$, as in Eq. (23). However, for consistency, we nevertheless always use Eq. (25) for the fitting and note that the case of a linear function of $1/L$ is encompassed by Eq. (25) with $\gamma=1$.

The extrapolated results for $\langle B \rangle^\infty$, plotted as a function of J_2, are shown in Fig. 10. For $J_2=0$ to $J_2^{c(1)}$, $\langle B \rangle^\infty$ is very small, even falling off from the small finite value at $J_2=0$, which we have argued to come about due to numerical and extrapolation errors. Note that here, for $J_2 < J_2^{c(1)} \approx 1$, the phase is characterized as bond-order wave within bosonization. While this seems to be a contradiction at first glance, note that the charge gap, Fig. 8, falls off very rapidly from its small finite value at $J_2=0$, whereas the spin gap opens very slowly due to its putative exponential form. In consequence,

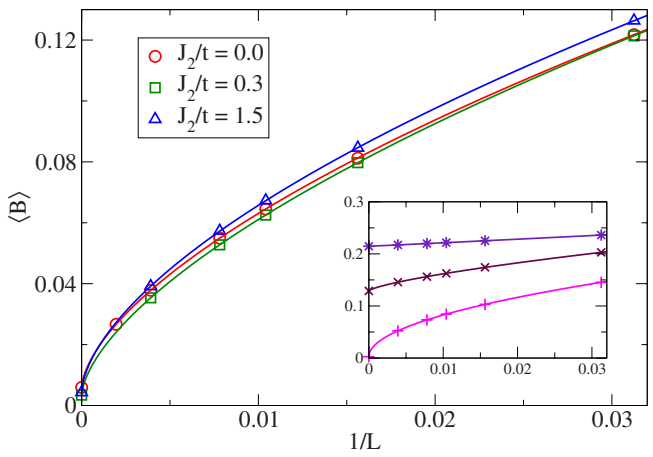

FIG. 9. (Color online) Finite-size scaling analysis for $\langle B \rangle(L)$ for different J_2 when $U=0$ and $J_1=1$. The inset shows the finite-size scaling analysis for $J_2=2.0$, 2.5, and 3.0, from bottom to top.

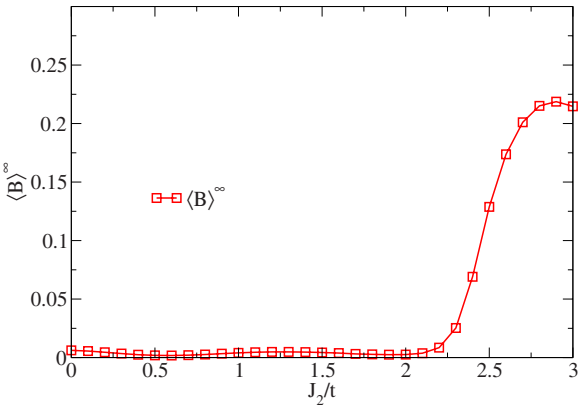

FIG. 10. (Color online) The $L=\infty$ extrapolated bond-order parameter $\langle B \rangle^\infty$ as a function of J_2 for $U=0$ and $J_1=1$.

the value of $\langle B \rangle^\infty$ is very small. Our interpretation, then is that the BOW order parameter is finite, but numerically unresolvable in this region. For $J_2^{c(1)} < J_2 < J_2^{c(2)}$, the spin gap is clearly nonvanishing, but $\langle B \rangle^\infty$ is numerically zero. This behavior is consistent with the bosonization prediction of a Luther-Emery phase. In other words, the vanishing charge gap indicates a phase in which there is no BOW. When $J_2 > J_2^{c(2)}$, coincident with the reopening of the charge gap in Fig. 8, the BOW phase reappears, this time clearly marked by a finite bond-order parameter as well as finite spin and charge gaps.

C. Results for nonzero U and J_2

We now study the effect of the frustration J_2 when the Coulomb repulsion U is finite. Bosonization predicts that the SDW phase that is present only along the $J_2=0$ line at $U=0$ becomes enlarged to a finite region at finite U. We explore the behavior as a function of J_2 for moderate values of U and J_1, $U=2$ and $J_1=1$.

Figure 11 shows the spin and charge gaps, extrapolated to infinite system size, a functions of J_2. As can be seen, the spin gap opens at a finite $J_2^s \approx 0.6$ and the charge gap, although at first decreasing and reaching a minimum at J_2

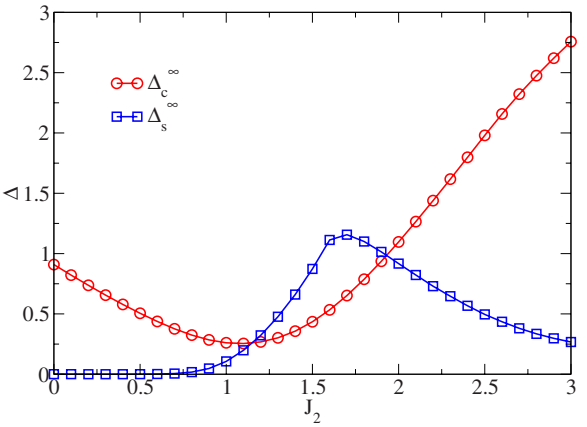

FIG. 11. (Color online) The $L=\infty$ extrapolated spin gap and charge gap as functions of J_2 for $U=2$, $J_1=1$.

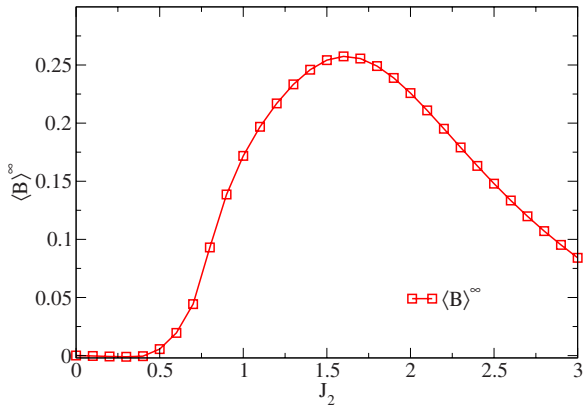

FIG. 12. (Color online) The $L=\infty$ extrapolated $\langle B\rangle$ as a function of J_2 for $U=2$, $J_1=1$.

≈ 1.1, is always finite. As can be seen in Fig. 12, the bond-order parameter $\langle B\rangle^{\infty}=0$ when $J_2<J_2^s$ and opens rapidly to a large, finite value at $J_2\approx 0.5$. The behavior of all quantities is consistent with a SDW phase for small J_2 and a BOW for large J_2. Bosonization does predict a transition from a SDW phase to a BOW phase at $J_2=U/2$ (see Fig. 2). However, it also predicts a transition to a spin-gapless LE phase at larger J_2, which is not found in the numerical calculations. In our opinion, this is because the values of U, J_1, and J_2 here are large enough so that the regime of validity of bosonization is exceeded. Note that the critical value $J_2^s\approx 0.5$ is far from the weak-coupling prediction of $J_2=U/2=2$, but agrees fairly well with the value expected from the frustrated Heisenberg chain, for which $(J_2^{\mathrm{Heis}}/J_1^{\mathrm{Heis}})_c\approx 0.241$,[26,27] if we take $J_1^{\mathrm{Heis}}=J_1+4t^2/U=3$, the effective Heisenberg coupling within strong coupling; this yields an estimate $J_2^{c(\mathrm{strong})}\approx 0.72$, in reasonable agreement with the DMRG result.

Figure 13 summarizes the phase diagrams as a function of J_2 obtained from the DMRG calculations at zero and finite U. For $U=0$, the SDW phase at $J_2=0$ becomes a BOW phase at arbitrarily small but weak J_2. At intermediate J_2, a metallic, but spin-gapped Luther-Emery phase occurs, and at large

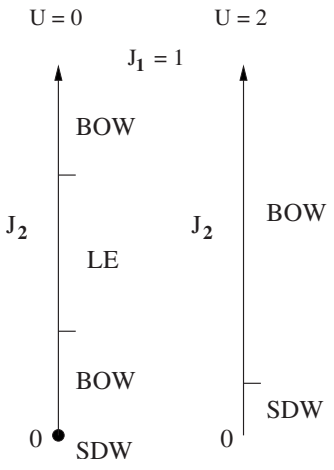

FIG. 13. A sketch of the ground-state phase diagram of the one-dimensional t-U-J_1-J_2 model at zero and finite U obtained from analysis of the DMRG calculations.

J_2 the system re-enters the BOW phase. At moderate, finite U, the SDW phase persists when J_2 is small and finite, going over to a BOW at larger J_2.

IV. DISCUSSION AND CONCLUSION

In this work, we have investigated the ground-state behavior of the one-dimensional Hubbard model at half band filling with antiferromagnetic nearest-neighbor and next-nearest-neighbor Heisenberg interactions. Our field-theoretical analysis for weak couplings indicates that the ground state has a finite gap for either charge excitations (spin-density-wave phase) or spin excitations (Luther-Emery phase) or both (bond-order-wave phase). Our extensive numerical DMRG investigations agree very well with the field-theoretical predictions for small interactions. The only exception is the lack of numerical evidence for a finite bond-order parameter in the region $U=0$, $J_1=1$, and $0<J_2<J_1$. Here the system sizes are large enough to resolve finite spin and charge gaps but they are still too small to detect the very small bond-order parameter.

For larger interactions, e.g., $U=2$, the DMRG finds a strong-coupling bond-order-wave phase which eludes the field-theoretical description. Instead, its existence and its properties can be inferred from a strong-coupling expansion of the model where it is seen that the strong-coupling BOW phase results from the frustration of the nearest-neighbor and next-nearest-neighbor Heisenberg couplings. Therefore, the metallic Luther-Emery phase is limited to a narrow weak-coupling region in the phase space where it would be very difficult to justify the strengths of the coupling parameters from microscopic considerations. For moderate interactions, an echo of the weak-coupling Luther-Emery phase can be seen in the behavior of the charge gap as a function of J_2, which displays a minimum at some $J_2\gtrsim J_1$.

The nearest-neighbor Heisenberg coupling J_1 is *not* a frustrating interaction for the half-filled Hubbard model because the ground state of the t-U-J_1 model is a spin-density wave for all $J_1\geq 0$. In order to arrive at this conclusion in the field-theoretical analysis, the fact that bosonic phase fields are locked to their mean-field values when excitations are gapped so that seemingly irrelevant operators become marginal operators, must be taken into account. In numerical calculations one needs to study rather large system sizes in order to extrapolate to a vanishing spin gap and bond-order parameter in the thermodynamic limit. The next-nearest-neighbor Heisenberg interaction J_2, in contrast, truly frustrates the Hubbard model, opening the way to Luther-Emery and bond-charge-ordered phases for $J_2>0$. As expected from our experience with the frustrated Heisenberg model, the SDW phase is stable against weak frustration for $U>0$, i.e., a finite J_2 is required to open the spin gap.

In conclusion, our study demonstrates both analytically and numerically that a nearest-neighbor Heisenberg exchange interaction added to the half-filled Hubbard model does not lead to frustration or to new phases in the ground-state phase diagram, whereas a frustrating next-nearest-neighbor exchange does.

ACKNOWLEDGMENTS

This work was partly supported by the Hungarian Research Fund (OTKA) Grant No. K-68340 and by the DFG-OTKA International Research Training Group 790 *Electron-Electron Interactions in Solids*.

[1] E. H. Lieb and F. Y. Wu, Phys. Rev. Lett. **20**, 1445 (1968); **21**, 192(E) (1968).
[2] *Conjugated Conducting Polymers*, Springer Series in Solid-State Sciences Vol. 102, edited by H. Kiess (Springer, Berlin, 1982).
[3] Y. J. Kim, J. P. Hill, H. Benthien, F. H. L. Essler, E. Jeckelmann *et al.*, Phys. Rev. Lett. **92**, 137402 (2004).
[4] H. Benthien, F. Gebhard, and E. Jeckelmann, Phys. Rev. Lett. **92**, 256401 (2004).
[5] M. Nakamura, J. Phys. Soc. Jpn. **68**, 3123 (1999); Phys. Rev. B **61**, 16377 (2000).
[6] A. W. Sandvik, L. Balents, and D. K. Campbell, Phys. Rev. Lett. **92**, 236401 (2004).
[7] M. Fabrizio, A. O. Gogolin, and A. A. Nersesyan, Phys. Rev. Lett. **83**, 2014 (1999).
[8] S. R. Manmana, V. Meden, R. M. Noack, and K. Schönhammer, Phys. Rev. B **70**, 155115 (2004).
[9] M. Fabrizio, Phys. Rev. B **54**, 10054 (1996).
[10] S. Daul and R. M. Noack, Phys. Rev. B **61**, 1646 (2000).
[11] P. W. Anderson, Phys. Rev. **124**, 41 (1961).
[12] B. A. Bernevig, R. B. Laughlin, and D. I. Santiago, Phys. Rev. Lett. **91**, 147003 (2003).
[13] L. Arrachea and D. Zanchi, Phys. Rev. B **71**, 064519 (2005).
[14] G. I. Japaridze and E. Müller-Hartmann, Phys. Rev. B **61**, 9019 (2000).
[15] J. Dai, X. Feng, T. Xiang, and Y. Yu, Phys. Rev. B **70**, 064518 (2004).
[16] X. Feng, Z. Xu, and J. Dai, J. Phys.: Condens. Matter **16**, 4245 (2004).
[17] A. A. Aligia and L. Arrachea, Phys. Rev. B **60**, 15332 (1999).
[18] J. Sólyom, Adv. Phys. **28**, 201 (1979).
[19] M. Tsuchiizu and A. Furusaki, Phys. Rev. Lett. **88**, 056402 (2002); Phys. Rev. B **69**, 035103 (2004).
[20] A. Gogolin, A. Nersesyan, and A. Tsvelik, *Bosonization and Strongly Correlated Systems* (Cambridge University Press, Cambridge, 1998).
[21] S. R. White, Phys. Rev. Lett. **69**, 2863 (1992); Phys. Rev. B **48**, 10345 (1993).
[22] *Density Matrix Renormalization: A New Numerical Method in Physics*, edited by I. Peschel, X. Wang, M. Kaulke, and K. Hallberg (Springer-Verlag, Berlin, 1999).
[23] U. Schollwöck, Rev. Mod. Phys. **77**, 259 (2005).
[24] T. Giamarchi, *Quantum Physics in One Dimension* (Oxford University Press, New York, 2004), Chap. 10.
[25] A. A. Ovchinnikov, Zh. Eksp. Teor. Fiz. **57**, 2137 (1969) [Sov. Phys. JETP **30**, 1160 (1970)].
[26] S. Eggert, Phys. Rev. B **54**, R9612 (1996).
[27] K. Okamoto and K. Nomura, Phys. Lett. A **169**, 433 (1992).